Automatic Detection of Distal Humerus Features: First Steps

José Negrillo-Cárdenas, Juan-Roberto Jiménez-Pérez and Francisco R. Feito
Graphics and Geomatics Group of Jaén, University of Jaén, Campus Las Lagunillas S/N, Jaén, Spain

Keywords: Bone, Humerus, Feature Detection, Landmark Detection, Geometrical Approach, Spatial Decomposition.

Abstract: Identification of specific landmarks in tissues is fundamental for understanding the human anatomy in medical applications. Specifically, the assessment of bone features allows to detect several pathologies in orthopedics. The recognition has been formerly carried out via visual identification, providing insufficient accuracy. Automatic solutions are required to improve the precision and minimize diagnostic and surgical planning time. In this paper, we study distal humerus landmarks and a new algorithm to automatically detect them in a reasonable time. Our technique does not require a prior training, as a geometrical approach with a spatial decomposition is used to explore several regions of interest of the bone. Finally, a set of experiments are performed, showing promising results.

1 INTRODUCTION

Improving the detection of specific tissues, pathologies, illnesses, etc. is one of the main goals of the fruitful relationship between medicine and computer graphics research fields (Vidal et al., 2006). Medical images represent a classic and effective instrument to advance in the achievement of this goal. The identification of bone features is relevant to a better comprehension of the musculo-skeletal system, to diagnose some diseases, to plan a bone fracture reduction or to design patient specific implants (Brownhill et al., 2007; Ron et al., 2002). In the special case of a joint, the right alignment between bones guarantees an adequate degree of freedom to move. As a result, identifying the corresponding 3D anatomical landmarks in each bone is the main target. A visual identification of these characteristics is not precise enough, as Brownhill et al. (2006) demonstrate in the case of the elbow. Consequently, computer guided or fully automatic approaches are required.

In this work in progress we present an automatic detection of humeral landmarks using a geometrical approach and spatial decomposition. Our proposal requires no user interaction from a mesh model of a humerus. We design a technique for each of the defined landmarks.

The paper is organized as follows: Section 2 overviews related work regarding automatic detection of landmarks with special focus on joints. Section 3 describes the anatomy of humerus. Section 4 details our proposal. Section 5 shows preliminary results. Finally, in section 6 we detail future work and our conclusions.

2 PREVIOUS WORK

This review focuses on automatic detection of landmarks. Landmark detection techniques have been used throughout the study of different pathologies in general medicine. Barbu et al. (2010) evaluate the lymph node size as an indicator of the evolution of a cancer treatment. Artificial intelligence can label organs in an automatic way using machine learning techniques. Han et al. (2015) classify several brain regions using multi-resolution regression. Kim et al. (2017) propose a supervised machine learning approach to automatically localize the left ventricle center point and the anterior right ventricle insertion point. Yefeng Zheng et al. (2012) present a discriminative learning algorithm to segment eight aortic valve landmarks from a C-arm computed tomography. In orthopedics, Yang et al. (2015) applied convolutional neural networks and Baek et al. (2013) statistical models to predict femoral landmarks.

Geometrical approaches give also accurate results without any kind of prediction. In general, they are more computer-demanding, but a previous training stage becomes unnecessary. A simple spatial

Negrillo-Cárdenas, J., Jiménez-Pérez, J. and Feito, F.
Automatic Detection of Distal Humerus Features: First Steps.
DOI: 10.5220/0007686103540359
In *Proceedings of the 14th International Joint Conference on Computer Vision, Imaging and Computer Graphics Theory and Applications (VISIGRAPP 2019)*, pages 354-359
ISBN: 978-989-758-354-4

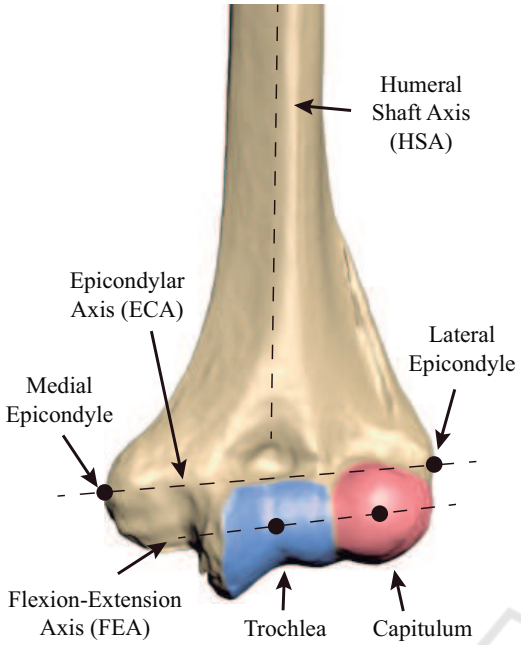

Figure 1: A visual representation of the most representative landmarks in a healthy distal humerus.

decomposition can be used to efficiently detect landmarks in specific bones. Subburaj et al. (2009) detect tibial features by curvature and spatial adjacency assessment. McDonald et al. (2009) determined a set of features in humerus to underpin an adequate alignment of the elbow joint. However, they provide insufficient technical details about how landmarks were obtained.

3 ANATOMY OF THE DISTAL HUMERUS

The humerus is a bone situated in the arm that connects shoulder and elbow. It is divided into three parts. The humeral head is the rounded upper region that allocates the shoulder. A long, cylindrical body determines the arm direction. The most distal part determines the elbow joint, that is composed of the humeroulnar and humeroradial joints. They allow the arm to be extended from 0 to 180^{o} in a healthy person (Delgado Martínez, 2015).

Distal humeral width is commonly defined as the distance between medial and lateral epicondyles (also known as epicondylar distance). Finally, the lowest part of the humerus contains several hollows, adapting it to ulna and radius. Figure 1 shows several points of interest: trochlea, capitulum, coronoid and olecranon. We refer the reader to An (2018); Shiba et al. (1988); London (1981) for further details regarding anatomy and biomechanical behavior of the elbow.

Apart from the referred anatomical features, several geometric landmarks can be established in order to improve diagnosis and to compare between other humeri. According to McDonald et al. (2009), humeral shaft axis (HSA) is defined as a line along the humerus, representing the geometric centers of distal and proximal endosteal canals. Epicondylar axis (ECA) is also designated as the line through medial and lateral epicondyles. An orthonormal reference coordinate system is defined with them, being the direction of HSA as up vector. The cross product of HSA and ECA represent $front$ and $up \times front$ determines the *right* orientation of the humerus. Note that *right* is the re-orthonormalization of ECA. Finally, the flexion-extension axis (FEA) is calculated to represent the direction of the elbow joint.

4 DETECTION OF LANDMARKS

Automatic detection of features is critical to significantly save processing time. Thus, manual placement becomes unnecessary to correctly situate the landmarks.

Our technique recognizes anatomical landmarks by using a geometric approach with spatial decomposition. Initially, a triangle mesh is generated from CT images using a classical *Marching cubes* algorithm (Lorensen and Cline, 1987). Afterwards the resulting mesh is simplified to reduce geometry

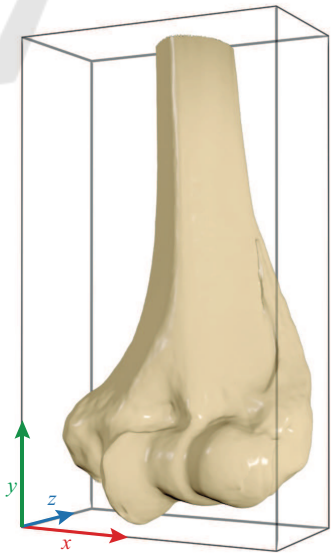

Figure 2: Reference coordinate axes of a humerus with its oriented bounding box.

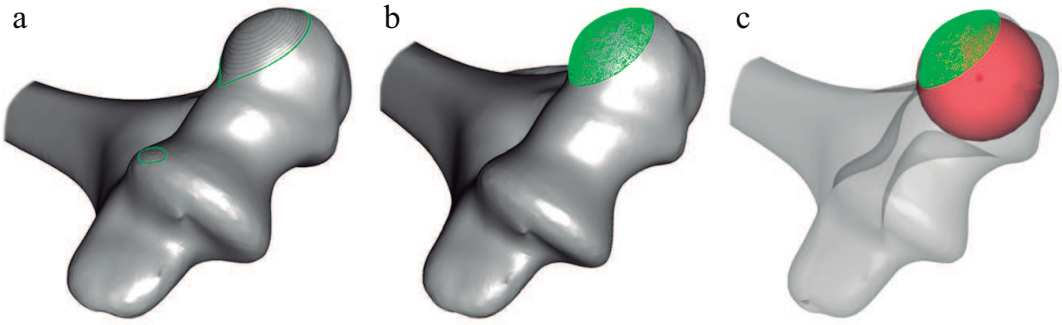

Figure 3: Steps to detect the center of a capitulum: (a) iterative cutting, (b) point cloud of the spherical cap, (c) approximated sphere (bone opacity is reduced to improve visualization).

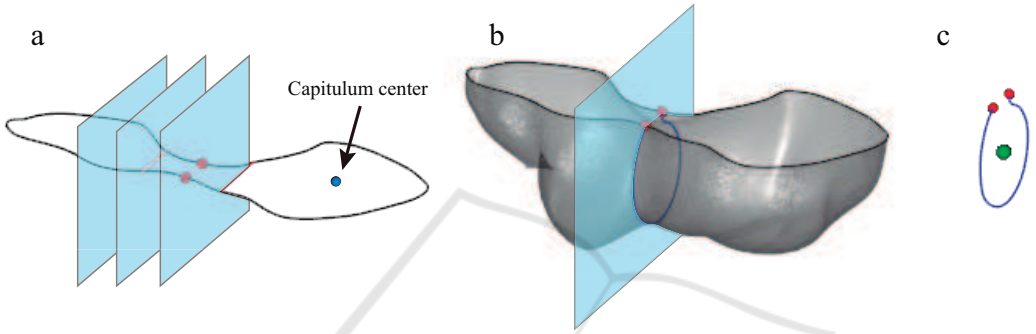

Figure 4: Steps to detect the center of the trochlea: (a) an iterative cutting of a slice containing the capitulum center, (b) new cutting plane through local minimum of the medial zone, (c) approximated circle center.

using a decimation filter. In addition, a Laplacian smoothing filter is applied in order to reduce irregularities of the resulting mesh due to the noise of initial medical images.

A detection of the initial orientation is necessary to explore the spatial structure of the bone. By employing a geometrical approach, we consider the direction of a humerus as the longest side of its oriented bounding box (OBB). In this manner, the middle-sized edge corresponds to width, and the shortest, to depth of the 3D model. Geometric operations are performed using the OBB edge directions as a reference coordinate system. Then, x, y, z vectors define the orientation of the bone (see Figure 2).

As mentioned before, humeral shaft axis represents a line along the proximal endosteal canal of the humerus. This axis is obtained by intersecting the upper humerus to a set of manually determined planes parallel to the bottom of the OBB. Finally, HSA is defined as a linear approximation of the mass centers of each slice, applying three-dimensional orthogonal regression (Schneider and Eberly, 2003).

Medial and lateral epicondyles are computed as tangent points of both flanking planes of the OBB, i.e., those parallel to the yz face as it is shown in Figure 2. However, the use of irregular meshes provoked by low-quality medical images may cause unpredictable behaviour and void results. Epsilon-based operations overcome this problem by adding an inner offset to the original planes. Finally, epicondylar axis is defined by connecting both detected points.

The calculation of HSA and ECA is thus resolved as it has been commented previously. However, detection of other regions of interest is not fully concluded in an automated way. McDonald et al. (2009) also studied the detection of capitulum and trochlea by using sphere and circle fit, respectively, in predefined areas. They do not provide sufficient details about the method for establishing the zones. Accordingly, in this work in progress, we identified without any kind of interaction the centers of trochlea and capitulum, by splitting distal humerus with a set of planes.

Anatomy of distal humerus shows the capitulum as a sphere at the end of the bone (Kawanishi et al., 2013). An iterative cutting is required to find a spherical cap. The process is stopped when two polygons are encountered at least. The mesh above the plane represents a point cloud in where a sphere can be fitted using a least squares method (Eberly, 2000). As a result, the origin of the sphere is an accurate approximation of the capitulum center, as it

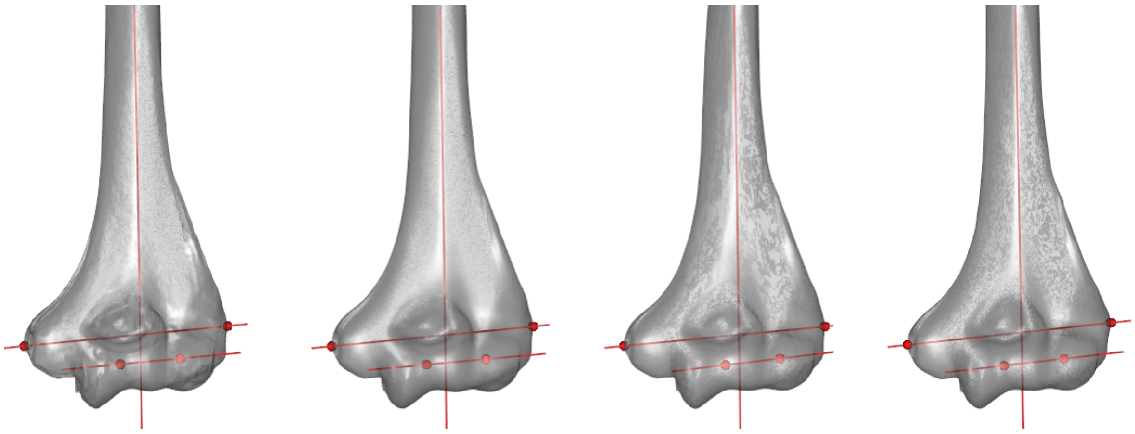

Figure 5: Landmarks detected in four humeri. Results are visually accurate.

is shown in Figure 3.

Trochlear sulcus is centered in distal humerus, next to the capitulum. It contains a groove to adapt the humerus to both ulna and radius. The center of the trochlea is placed approximately at the same height as the center of the capitulum. Thus, a cutting plane containing it, parallel to the bottom of the OBB, is defined. The clip function results a polygon representing the contour of the slice (Figure 4.a). Due to the trochlear and olecranon sulcus, a narrowing zone contains the center of the trochlea. The desired zone can be detected by minimizing the medial section of this polygon. Finally, an orthogonal plane to this minimum section is defined to slice the most distal part of the humerus (Figure 4.b). The least squares circle fitting algorithm (Eberly, 2000) is applied to the resulting strip to detect the requested point (see Figure 4.c).

To conclude, the flexion-extension axis (FEA) is defined by the connection of trochlea and capitulum centers.

5 EXPERIMENTS AND RESULTS

This section details the experiments performed to determine the validity of our method.

A set of four phantom humeri were scanned using a structured light 3D scanner Artec Eva[1]. Distal part of each one was registered and 3D meshes were generated using Artec Studio Professional software.

A program based on The Visualization Toolkit, VTK (Schroeder et al., 2006) was used to implement and test our algorithm. Currently, we calculated the following points of interest for each bone:

- Trochlea center.
- Capitulum center.
- Lateral epicondyle.
- Medial epicondyle.
- Humeral shaft axis.
- Epicondylar axis.
- Flexion-extension axis.

Currently, results are visually satisfactory (Figure 5), as they match with human atlas of anatomy (Rohen et al., 2011). Further testing is required to compare between results and ensure a robust algorithm in different situations.

5.1 Current Issues

As mentioned in Section 4, a correct initial orientation of the bone is critical to properly apply a spatial decomposition.

VTK constructs an OBB using a classical approach (Gottschalk et al., 1996). Mean of the vertices and a covariance matrix are calculated. Then, three eigenvectors define the bounding box edges. Nevertheless, they depend on initial geometry and orientation of the mesh, producing invalid results for our algorithm in some cases. In other words, the reference corner of the OBB is placed differently depending on models used. When an initial orientation and a corner are predefined, our algorithm runs as expected.

6 CONCLUSIONS

We have described an automatic feature detection algorithm for distal humeri from surface models. This approach can be applied to detect some anomalies in a bone or treat pathologies. Our technique has

[1] https://www.artec3d.com/portable-3d-scanners/artec-eva

been based on a geometrical approach, using a spatial decomposition. We have accomplished our primary objective of obtaining bone landmarks in an efficient way, requesting no interaction. In this position, main issues of our algorithm have been also analyzed. Preliminary experiments show promising results in terms of accuracy and performance.

Currently, we are improving the robustness of the algorithm, solving mentioned problems in Section 5.1. For instance, current manual parameters should be dynamically established for each case. Further testing using additional models is required to obtain more detailed results (e.g., accuracy and CPU/memory usage).

ACKNOWLEDGEMENTS

Authors are part of Graphics and Geomatics Group of Jaén (TIC-144). This research was supported by the Spanish Ministry of Education, Culture and Sports via a doctoral grant to the first author (Ref. FPU16/01439) and partially by Spanish Ministry of Science, Innovation and Universities through research projects DPI2015-65123-R and TIN2017-84968-R.

REFERENCES

An, K.-N. (2018). Biomechanics of the Elbow. *Morrey's the Elbow and its Disorders*, pages 33–46.

Baek, S.-Y., Wang, J.-H., Song, I., Lee, K., Lee, J., and Koo, S. (2013). Automated bone landmarks prediction on the femur using anatomical deformation technique. *Computer-Aided Design*, 45(2):505–510.

Barbu, A., Suehling, M., Xu, X., Liu, D., Zhou, S. K., and Comaniciu, D. (2010). Automatic Detection and Segmentation of Axillary Lymph Nodes. In *Proceedings of the 13th International Conference on Medical Image Computing and Computer-assisted Intervention: Part I*, MICCAI'10, pages 28–36, Berlin, Heidelberg. Springer-Verlag.

Brownhill, J. R., Furukawa, K., Faber, K. J., Johnson, J. A., and King, G. J. (2006). Surgeon accuracy in the selection of the flexion-extension axis of the elbow: An in vitro study. *Journal of Shoulder and Elbow Surgery*, 15(4):451 – 456.

Brownhill, J. R., King, G. J., and Johnson, J. A. (2007). Morphologic analysis of the distal humerus with special interest in elbow implant sizing and alignment. *Journal of Shoulder and Elbow Surgery*, 16(3):S126–S132.

Delgado Martínez, A. (2015). *Cirugía Ortopédica y Traumatología*. Editorial Médica Paramericana.

Eberly, D. H. (2000). *3D Game Engine Design: A Practical Approach to Real-time Computer Graphics*. Morgan Kaufmann Publishers Inc., San Francisco, CA, USA.

Gottschalk, S., Lin, M. C., and Manocha, D. (1996). OBBTree: A hierarchical structure for rapid interference detection. In Anon, editor, *Proceedings of the ACM SIGGRAPH Conference on Computer Graphics*, pages 171–180.

Han, D., Gao, Y., Wu, G., Yap, P.-T., and Shen, D. (2015). Robust anatomical landmark detection with application to MR brain image registration. *Computerized Medical Imaging and Graphics*, 46:277–290.

Kawanishi, Y., Miyake, J., Kataoka, T., Omori, S., Sugamoto, K., Yoshikawa, H., and Murase, T. (2013). Does cubitus varus cause morphologic and alignment changes in the elbow joint? *Journal of shoulder and elbow surgery*, 22(7):915–23.

Kim, Y.-C., Chung, Y., and Choe, Y. H. (2017). Automatic localization of anatomical landmarks in cardiac mr perfusion using random forests. *Biomedical Signal Processing and Control*, 38:370 – 378.

London, J. T. (1981). Kinematics of the elbow. *The Journal of bone and joint surgery. American volume*, 63(4):529–35.

Lorensen, W. E. and Cline, H. E. (1987). Marching cubes: A high resolution 3D surface construction algorithm. *Proceedings of the 14th annual conference on Computer graphics and interactive techniques - SIGGRAPH '87*, 21(4):163–169.

McDonald, C. P., Peters, T. M., King, G. J., and Johnson, J. A. (2009). Computer assisted surgery of the distal humerus can employ contralateral images for pre-operative planning, registration, and surgical intervention. *Journal of Shoulder and Elbow Surgery*, 18(3):469–477.

Rohen, J. W., Yokochi, C., and Lütjen-Drecoll, E. (2011). *Color Atlas of Anatomy: A Photographic Study of the Human Body*. Wolters Kluwer, Lippincott Williams & Wilkins, 7 edition.

Ron, O., Joskowicz, L., Milgrom, C., and Simkin, A. (2002). Computer-based periaxial rotation measurement for aligning fractured femur fragments from CT: A feasibility study. *Computer Aided Surgery*, 7(6):332–341.

Schneider, P. J. and Eberly, D. H. (2003). *Geometric Tools for Computer Graphics*. Elsevier.

Schroeder, W., Martin, K., and Lorensen, B. (2006). *The Visualization Toolkit–An Object-Oriented Approach To 3D Graphics*. Kitware, Inc., fourth edition.

Shiba, R., Sorbie, C., Siu, D. W., Bryant, J. T., Cooke, T. D. V., and Wevers, H. W. (1988). Geometry of the humeroulnar joint. *Journal of Orthopaedic Research*, 6(6):897–906.

Subburaj, K., Ravi, B., and Agarwal, M. (2009). Automated identification of anatomical landmarks on 3D bone models reconstructed from CT scan images. *Computerized Medical Imaging and Graphics*, 33(5):359–368.

Vidal, F., Bello, F., Brodlie, K., John, N., Gould, D., Phillips, R., and Avis, N. (2006). Principles and Applications of Computer Graphics in Medicine. *Computer Graphics Forum*, 25(1):113–137.

Yang, D., Zhang, S., Yan, Z., Tan, C., Li, K., and Metaxas, D. (2015). Automated anatomical landmark detection ondistal femur surface using convolutional neural network. In *2015 IEEE 12th International Symposium on Biomedical Imaging (ISBI)*, pages 17–21. IEEE.

Yefeng Zheng, John, M., Rui Liao, Nottling, A., Boese, J., Kempfert, J., Walther, T., Brockmann, G., and Comaniciu, D. (2012). Automatic Aorta Segmentation and Valve Landmark Detection in C-Arm CT for Transcatheter Aortic Valve Implantation. *IEEE Transactions on Medical Imaging*, 31(12):2307–2321.